# Alterations in action potential profile enhance excitation–contraction coupling in rat cardiac myocytes

Rajan Sah, Rafael J. Ramirez, Roger Kaprielian and Peter H. Backx

*Toronto General Hospital, CCRW 3-802, 101 College Street, Toronto, Ontario, Canada M5G 2C4*

(Received 9 October 2000; accepted after revision 17 January 2001)

1. Action potential (AP) prolongation typically occurs in heart disease due to reductions in transient outward potassium currents ($I_{to}$), and is associated with increased $Ca^{2+}$ transients. We investigated the underlying mechanisms responsible for enhanced $Ca^{2+}$ transients in normal isolated rat ventricular myocytes in response to the AP changes that occur following myocardial infarction.

2. Normal myocytes stimulated with a train of long post-myocardial infarction (MI) APs showed a 2.2-fold elevation of the peak $Ca^{2+}$ transient and a 2.7-fold augmentation of fractional cell shortening, relative to myocytes stimulated with a short control AP.

3. The steady-state $Ca^{2+}$ load of the sarcoplasmic reticulum (SR) was increased 2.0-fold when myocytes were stimulated with trains of long post-MI APs ($111 \pm 21.6$ $\mu$mol $l^{-1}$) compared with short control APs ($56 \pm 7.2$ $\mu$mol $l^{-1}$).

4. Under conditions of equal SR $Ca^{2+}$ load, long post-MI APs still resulted in a 1.7-fold increase in peak $[Ca^{2+}]_i$ and a 3.8-fold increase in fractional cell shortening relative to short control APs, establishing that changes in the triggering of SR $Ca^{2+}$ release are largely responsible for elevated $Ca^{2+}$ transients following AP prolongation.

5. Fractional SR $Ca^{2+}$ release calculated from the measured SR $Ca^{2+}$ load and the integrated SR $Ca^{2+}$ fluxes was $24 \pm 3$ and $11 \pm 2$% following post-MI and control APs, respectively.

6. The fractional release (FR) of $Ca^{2+}$ from the SR divided by the integrated L-type $Ca^{2+}$ flux ($FR/\int F_{Ca,L}$) was increased 1.2-fold by post-MI APs compared with control APs. Similar increases in excitation–contraction (E–C) coupling gains were observed establishing enhanced E–C coupling efficiency.

7. Our findings demonstrate that AP prolongation alone can markedly enhance E–C coupling in normal myocytes through increases in the L-type $Ca^{2+}$ current ($I_{Ca,L}$) trigger combined with modest enhancements in $Ca^{2+}$ release efficiency. We propose that such changes in AP profile in diseased myocardium may contribute significantly to alterations in E–C coupling independent of other biochemical or genetic changes.

Action potential (AP) prolongation is universally observed in human patients with heart disease as well as in several animal models as a result of a reduction in the expression of potassium channel genes *Kv4.2* and *Kv4.3* which encode the channels for the transient outward current ($I_{to}$) (Beuckelmann *et al.* 1993; Brooksby *et al.* 1993; Cerbai *et al.* 1994; Kaab *et al.* 1996; Wickenden *et al.* 1998; Kaprielian *et al.* 1999). We and others have shown previously that this AP prolongation results in elevated $[Ca^{2+}]_i$ (Bouchard *et al.* 1995; Wickenden *et al.* 1998; Kaprielian *et al.* 1999) which enhances contractility of compromised myocardium (Fiset *et al.* 1997). The increase in $Ca^{2+}$ transients and contractility observed following AP prolongation may be explained by an enhanced triggered sarcoplasmic reticulum (SR) $Ca^{2+}$ release, an elevated SR $Ca^{2+}$ load or both. Previous studies have attributed increases in inotropy following AP prolongation to elevations in SR $Ca^{2+}$ load (Brooksby *et al.* 1993; Bouchard *et al.* 1995). Changes in SR $Ca^{2+}$ load have also been shown to influence the efficiency of SR $Ca^{2+}$ release (Han *et al.* 1994; Janczewski *et al.* 1995; Santana *et al.* 1997) although these studies used step depolarizations to trigger $Ca^{2+}$ release rather than APs. On the other hand, elevations in SR $Ca^{2+}$ release have also been linked to increases in L-type $Ca^{2+}$ current ($I_{Ca,L}$) trigger. Specifically, prolongation of step depolarization duration, particularly in the range 2–20 ms, enhanced SR $Ca^{2+}$ release independently of SR $Ca^{2+}$ load by increasing the $I_{Ca,L}$ trigger (Isenberg & Han, 1994). This strong dependence of SR $Ca^{2+}$ release on step duration suggests

that a similar mechanism may underlie altered $Ca^{2+}$ release in heart disease since the early repolarization phase of the AP, and the corresponding temporal changes in $I_{Ca,L}$, are primarily affected by $I_{to}$ reductions (Kaprielian *et al.* 1999).

Recently, changes in E–C coupling efficiency have been reported in different animal models of hypertensive heart disease, with one study reporting enhanced SR $Ca^{2+}$ release (Shorofsky *et al.* 1999) and another finding impaired release (Gomez *et al.* 1997). Unfortunately neither of these studies took into account the possible effects of AP prolongation that are known to occur in spontaneous hypertensive rats (Brooksby *et al.* 1993; Cerbai *et al.* 1994). This is particularly relevant since AP prolongation in spontaneous hypertensive rats (Brooksby *et al.* 1993) and in rats following myocardial infarction has been directly linked to increased $Ca^{2+}$ transient amplitudes, although the underlying mechanism for these changes was not thoroughly investigated. In addition, based on previous studies demonstrating $I_{Ca,L}$-independent forms of SR $Ca^{2+}$ release such as $Na^+$–$Ca^{2+}$ exchange-mediated release (Levesque *et al.* 1991; Wasserstrom & Vites, 1996; Sipido *et al.* 1997; Litwin *et al.* 1998) and voltage-sensitive release (Ferrier *et al.* 1998; Howlett *et al.* 1998), one might anticipate that prolonged APs might also alter the efficiency of $Ca^{2+}$ release.

This study was designed to determine the mechanism for the changes in $Ca^{2+}$ transients associated specifically with AP prolongation observed following myocardial infarction in terms of changes in trigger $I_{Ca,L}$ versus changes in SR $Ca^{2+}$ load. We find that when normal myocytes are stimulated with prolonged action potentials, positive inotropic effects are mediated primarily through an increase in triggered $Ca^{2+}$ release and are secondarily due to an enhancement in SR $Ca^{2+}$ load. This elevated $Ca^{2+}$ release appears to result primarily from increased $Ca^{2+}$ influx mediated by $I_{Ca,L}$ combined with a modest enhancement in the efficiency of $Ca^{2+}$ release evoked by post-MI APs.

## METHODS

### Isolation of rat ventricular myocytes

The procedure for isolation of adult rat ventricular myocytes was adapted from our previous studies (Wickenden *et al.* 1997). Male Sprague-Dawley rats (300–400 g, Charles River) were heparinized and killed by intraperitoneal injection of a lethal dose of anaesthetic (sodium pentobarbital, 200 mg $kg^{-1}$) in accordance with the Guidelines of the Animal Care and Use Committee of the University Health Network. Hearts were cannulated and retrogradely perfused through the aorta for about 1 min with a $Ca^{2+}$-containing standard Tyrode solution (mM): 140 NaCl, 5.4 KCl, 10 Hepes, 1 $MgCl_2$, 1 $CaCl_2$ and 10 D-glucose, adjusted to pH 7.4 with NaOH at 37 °C. The hearts were then perfused with nominally $Ca^{2+}$-free standard Tyrode solution for 5 min prior to digestion with the same solution containing collagenase (Type II, 0.38 mg $ml^{-1}$, Boehringer-Mannheim) and protease (Type XIV, 0.03 mg $ml^{-1}$, Sigma) for 8–9 min. The enzyme solution was then washed out by perfusing for 2–3 min with a Kraft-Brühe (high $K^+$) solution (mM): 120 potassium glutamate, 20 KCl, 10 Hepes, 1 $MgCl_2$, 0.3 K-EGTA and 10 D-glucose, pH 7.4. All solutions were pre-bubbled with 100 % $O_2$ for 5 min. Following the enzyme washout, the atria and blood vessels were removed and ventricles separated. The right and left ventricular free walls were dissected from the remainder of the heart. Myocytes were minced and mechanically dissociated in high $K^+$ solution and then filtered through a nylon mesh. The cells were then resuspended in high $K^+$ solution containing bovine serum albumin (0.04 % w/v) and gentamycin (0.05 mg $ml^{-1}$) and used within 12 h after isolation. Only $Ca^{2+}$-tolerent, quiescent, rod-shaped myocytes with clear cross-striations were selected for electrophysiological, intracellular $Ca^{2+}$ and unloaded cell shortening measurements.

### Intracellular $Ca^{2+}$ and cell shortening measurements during AP clamps

Freshly isolated rat ventricular myocytes were placed in a bath on the stage of an Olympus IX50 inverted microscope and perfused at room temperature (20–23 °C at approximately 1 ml $min^{-1}$) with extracellular solution of the following composition (mM): 140 NaCl, 4 KCl, 10 Hepes, 1 $MgCl_2$, 2 $CaCl_2$ and 10 D-glucose, adjusted to 7.4 with NaOH. Myocytes were voltage clamped using the whole-cell patch clamp technique (Hamill *et al.* 1981) with an Axopatch 200A amplifier (Axon Instruments). Microelectrodes were pulled from thin-walled 1.5 mm diameter borosilicate glass (World Precision Instruments) using a Flaming-Brown micropipette puller (Sutter Instruments) and heat polished to a final resistance of 1–2 MΩ when filled with a solution containing (mM): 140 KCl, 10 Hepes, 1 $MgCl_2$, 10 NaCl, 7 MgATP, 0.060 fura-2 pentapotassium salt, adjusted to pH 7.2 with KOH. Series resistance compensation ranged between 80 and 90 %. Fluorescence measurements were performed using light from a 75 W xenon lamp (Oriel Corp., CT, USA) passed through bandpass filters centred at either 340 or 380 nm (Chromatech, VT, USA). The emitted fluorescence was collected by a ×40 Uapo/340 objective lens (Olympus America, Melville, NY, USA) and passed through a 510 nm filter to a photomultiplier tube (R2693, Hamamatsu, Japan). The photomultiplier output was filtered at 100 Hz, recorded using an A/D data acquisition board (Model PP-50 Warner, CT, USA) and stored in a computer for analysis. The ratio ($R$) of the background-subtracted fluorescence signal (340/380) was used to estimate $[Ca^{2+}]_i$ as described previously (Kaprielian *et al.* 1999). In our experiments $\beta$, which is defined as the ratioof fluorescence measured with 380 nm excitation light in the absence of $Ca^{2+}$ to that measured at saturating levels of $Ca^{2+}$ (10 mM), was $11.3 \pm 0.3$ ($n = 2$). The fluorescence ratio in the presence of saturating $Ca^{2+}$ ($R_{max}$) was $5.9 \pm 0.1$ ($n = 2$) and that in the absence of $Ca^{2+}$ ($R_{min}$) was $0.23 \pm 0.03$ ($n = 2$). Cells were stimulated with either step depolarizations or AP clamps using waveforms obtained from control and post-MI myocytes (Kaprielian *et al.* 1999). All $[Ca^{2+}]_i$ and cell shortening measurements were made under steady-state conditions following loading trains of these APs or 100 ms steps at a frequency of 0.25 Hz. To obtain a fluorescence measurement from both 340 and 380 nm excitation wavelengths, each protocol was repeated at least once. The reliability of using this approach was validated in several cells by repeated fluorescence measures at 340 and 380 nm excitation following the loading trains and the measurements proved to be stable throughout the duration of the experiment.

Unloaded cell shortening was measured simultaneously with fluorescence using a CCD video camera mounted on the sideport of the microscope. Custom-made relay lenses were installed in the

sideport to reduce the image of myocytes to fit into the active area of the camera. Raster lines were positioned over both edges of the myocyte and the focus and detection thresholds were adjusted to maximize the signal-to-noise ratio. Dual-edge motion was monitored by an edge-detection system (Crescent Electronics, Salt Lake City, UT, USA), digitized on-line and stored on a personal computer using pCLAMP software.

The fluorescence signals and cell motion signals were both digitized at 4 kHz. Cell motion was measured at 60 Hz, which is the acquisition rate of the CCD camera used. The fluorescence signals were filtered at 100 Hz.

### L-type $Ca^{2+}$ current during AP clamps

Calcium current and $Ca^{2+}$ transients were measured simultaneously during an AP clamp by eliminating $Na^+$ and $K^+$ currents followed by a $Cd^{2+}$ subtraction. Interfering $K^+$ currents were eliminated by replacing almost all intracellular and extracellular $K^+$ with $Cs^+$. The intracellular solution contained (mM): 140 CsCl, 2 KCl, 10 Hepes, 1 $MgCl_2$, 10 NaCl, 7 MgATP and 0.060 fura-2 pentapotassium salt, adjusted to pH 7.2 with CsOH. The extracellular solution contained (mM): 140 NaCl, 4 CsCl, 10 Hepes, 1 $MgCl_2$, 2 $CaCl_2$, 10 D-glucose and 30 $\mu$M TTX, pH 7.4 with NaOH. It was applied using a rapid local superfusion device (BMT Research Services, Calgary, Alberta, Canada). After $Ca^{2+}$ currents and transients were measured the extracellular solution was switched to one containing 500 $\mu$M $CdCl_2$ and the trace acquired was used for subtraction to eliminate all other background currents.

### Measurement of SR $Ca^{2+}$ load

SR $Ca^{2+}$ load was estimated following trains of either eight AP waveforms or 100 ms steps to 10 mV applied every 4 s to establish steady-state SR load conditions. After eight loading pulses the myocyte was rapidly superfused with standard Tyrode solution containing 20 mM caffeine. Application of caffeine caused myocyte contraction as a result of $Ca^{2+}$ release from the SR (Varro *et al.* 1993). Throughout the caffeine application the membrane potential was held at −80 mV to enhance $I_{Na-Ca}$ and thereby allowed estimation of the SR $Ca^{2+}$ content by integrating $I_{Na-Ca}$ over the duration of the caffeine application. Cell volume was calculated from the mean cell membrane capacitance (178 ± 7 pF, $n = 18$) and converted to volume by assuming a surface area to volume ratio of 0.5 $\mu m^{-1}$ (Page, 1978) and a specific capacity of 1 $\mu F\ cm^{-2}$. Calcium efflux via non-electrogenic pathways was corrected for by dividing by 0.87, in accordance with the findings of Bassani *et al.* (1994) that 87 % of the $Ca^{2+}$ flux during a caffeine contracture occurs through $Na^+$–$Ca^{2+}$ exchange.

### Computation of SR $Ca^{2+}$ flux, $F_{rel}$, and measurement of E–C coupling gain

The SR $Ca^{2+}$ release flux ($F_{rel}$) was determined from $Ca^{2+}$ transient recordings using the method of Wier *et al.* (1994). Calcium influx into the myoplasm via sarcolemmal $I_{Ca,L}$ is believed to contribute little to the amplitude of the $Ca^{2+}$ transient in the rat (Terracciano & MacLeod, 1997). Indeed, our calculations confirmed that $Ca^{2+}$ influx represents less than 6 % of the total $Ca^{2+}$ released (see below, Fig. 8*A*). Accordingly, the rate of change of $[Ca^{2+}]_i$ is almost entirely determined by the net flux of $Ca^{2+}$ across the SR membrane plus the binding and unbinding to intracellular ligands as given by:

$$d[Ca^{2+}]_{i,corr}/dt = F_{rel} + F_{pump} + F_{leak} + \sum d[CaL]/dt, \quad (1)$$

where $F_{rel}$ is the SR $Ca^{2+}$ release flux, $F_{pump}$ is the SR $Ca^{2+}$ uptake flux via the SR ATPase, $F_{leak}$ is the background $Ca^{2+}$ leak from the SR to the cytoplasm (fixed at 0.0175 mM $s^{-1}$; Balke *et al.* 1994), [CaL] is the concentration of ligand-bound $Ca^{2+}$ and d/d$t$ represents the first derivative with respect to time. For the purposes of SR $Ca^{2+}$ flux estimation, a corrected calcium transient ($[Ca^{2+}]_{i,corr}$) was calculated taking into account the kinetics of binding of $Ca^{2+}$ to fura-2 as described by Sipido & Wier (1991):

$$[Ca^{2+}]_{i,corr} = \frac{\beta\, dR/dt[1 - (R - R_{min})(\beta - 1)/((\beta - 1)R + R_{max} - \beta R_{min})] + k_{off}\beta(R - R_{min})}{k_{on}(R_{max} - R)}, \quad (2)$$

For this calculation the value of $k_{off}$ was taken to be 23 $s^{-1}$ (Baylor & Hollingworth, 1988) and $k_{on}$ was determined to be $1.03 \times 10^8$ $M^{-1}\ s^{-1}$ assuming a $K_D$ for fura-2 of 224 nM. The time derivative, $d[Ca^{2+}]_{i,corr}/dt$, is calculated from the corrected calcium transient recording in a three-point, sliding-window, linear model using a least squares estimator. The expressions for $F_{pump}$ (Balke *et al.* 1994) and d[CaL]/d$t$ (Sipido & Wier, 1991) were:

$$F_{pump} = -V_{max}/(1 + (K_m/[Ca^{2+}]_i)^4), \quad (3)$$

$$d[CaL]/dt = k^L_{on}[Ca^{2+}]_i([L]_{tot} - [CaL]) - k^L_{off}[CaL], \quad (4)$$

where $V_{max}$ is the maximal SR uptake flux defined as 0.2 mM $s^{-1}$ (Balke *et al.* 1994), L represents intracellular ligands including calmodulin, troponin and fura-2 and $k^L_{on}$ and $k^L_{off}$ are binding rate constants for the respective ligands. The affinity constant ($K_m$) was adjusted for each cell to eliminate baseline SR flux, as done previously (Wier *et al.* 1994). In nine cells, $K_m$ ranged from 0.09 to 0.31 $\mu$M with an average of 0.178 ± 0.006 $\mu$M, which is comparable to previously reported values (Balke *et al.* 1994).

Using these definitions, the SR $Ca^{2+}$ release flux ($F_{rel}$) can be obtained directly from the kinetically corrected $Ca^{2+}$ transient (eqn (2)) and eqn (1). The integral of $F_{rel}$ provides a measure of the amount of $Ca^{2+}$ released by the SR following an AP. An estimate of $Ca^{2+}$ influx responsible for triggering $Ca^{2+}$ release (i.e. $\int F_{Ca,L}$) was determined from the integrated $Ca^{2+}$ current according to:

$$\int F_{Ca,L} = 2\int_o^{peak} I_{Ca,L}dt/(zF \times 0.5V),$$

where $z$ is the valence of $Ca^{2+}$, $F$ is Faraday's constant ($9.648 \times 10^4$ C $mol^{-1}$), the factor 0.5 is the fraction of the total cell volume assumed to be accessible to $Ca^{2+}$ (Wier *et al.* 1994) and $V$ is the total cell volume calculated from the mean cell membrane capacitance (178 ± 7 pF, $n = 18$) as described above. The term $2\int_o^{peak} I_{Ca,L}dt$ represents twice the integrated $I_{Ca,L}$ from the baseline to the peak and reflects the contribution of first openings of L-type $Ca^{2+}$ channels (i.e. first latency distribution) to $I_{Ca,L}$ (Rose *et al.* 1992). Previous studies have established that the time course of $Ca^{2+}$ release coincides closely with the first latency of L-type $Ca^{2+}$ channel activation (Isenberg & Han, 1994; Lopez-Lopez *et al.* 1995; Sham *et al.* 1998; Cleemann *et al.* 1998; Collier *et al.* 1999) and that the $Ca^{2+}$ release correlates well with the cumulative probability density distribution of first latency of L-type $Ca^{2+}$ channels or the activation time course of the whole-cell $Ca^{2+}$ current (Isenberg & Han, 1994). Therefore, $2\int_o^{peak} I_{Ca,L}dt$ should provide an accurate estimate of the $Ca^{2+}$ influx that is responsible for triggering $Ca^{2+}$ release from the SR. It is important to point out that the values obtained using $2\int_o^{peak} I_{Ca,L}dt$ to measure trigger $Ca^{2+}$ are very similar to the integral of $I_{Ca,L}$ over the first 20 ms (i.e. $\int I_{Ca,20ms}dt$) which was previously suggested to provide a better measure of $I_{Ca,L}$ directly involved in the $Ca^{2+}$ release process (Fabiato, 1985; Janczewski *et al.* 1995).

Two definitions of E–C coupling gain were used to assess the efficiency of $Ca^{2+}$ release from the SR in our studies:

$$\text{E–C gain}_1 = \int F_{rel} / \int F_{Ca,L}$$

$$\text{E–C gain}_2 = \text{d(CS)}/\text{d}t / \int F_{Ca,L},$$

where $\int F_{rel}$ is the integrated SR $Ca^{2+}$ release flux or total SR $Ca^{2+}$ released, and d(CS)/d$t$ is the rate of cell shortening. These estimates of gain are similar to previous definitions of Wier *et al.* (1994) and Litwin *et al.* (1998) except that integrated fluxes are used instead of peak fluxes or peak current amplitudes. As a result, the E–C gain was calculated as a ratio of the total SR $Ca^{2+}$ release to the total trigger $Ca^{2+}$ influx. This modification was necessary since peak $I_{Ca,L}$ amplitude, which has previously been used as a measure of trigger $I_{Ca,L}$ during step depolarizations (Wier *et al.* 1994; Santana *et al.* 1997; Litwin *et al.* 1998), depends strongly on the AP profile (see below, Fig. 6) (Bouchard *et al.* 1995; Kaprielian *et al.* 1999).

From the calculated SR fluxes, another index of calcium release used in our studies was fractional release (FR), which was estimated as the integrated SR $Ca^{2+}$ flux divided by the measured total SR $Ca^{2+}$ content following a loading train of 100 ms steps ($\int F_{rel}$/total SR content).

### Data analysis

All data are presented as means ± S.E.M. with the number of cells in parentheses. Comparisons of data for each cell between long post-MI APs and short control APs were performed using Student's two-tailed, paired $t$ test. An unpaired $t$ test was used when comparing data that did not originate from the same myocyte. An experimental $P$ value $< 0.05$ was considered statistically significant.

## RESULTS

### Effects of the long post-MI AP profile on $[Ca^{2+}]_i$, cell shortening and SR load

In this study normal, freshly isolated rat cardiomyocytes were stimulated with either short control or long post-MI APs that had been previously recorded in myocytes derived from control or post-MI rats (Fig. 1*A*). In each case the SR was loaded to a steady-state level by introducing eight conditioning APs (Trafford *et al.* 1997) after which a test AP was applied. Figure 1*B* and *D* (left) shows that peak $Ca^{2+}$ transient magnitudes in response to

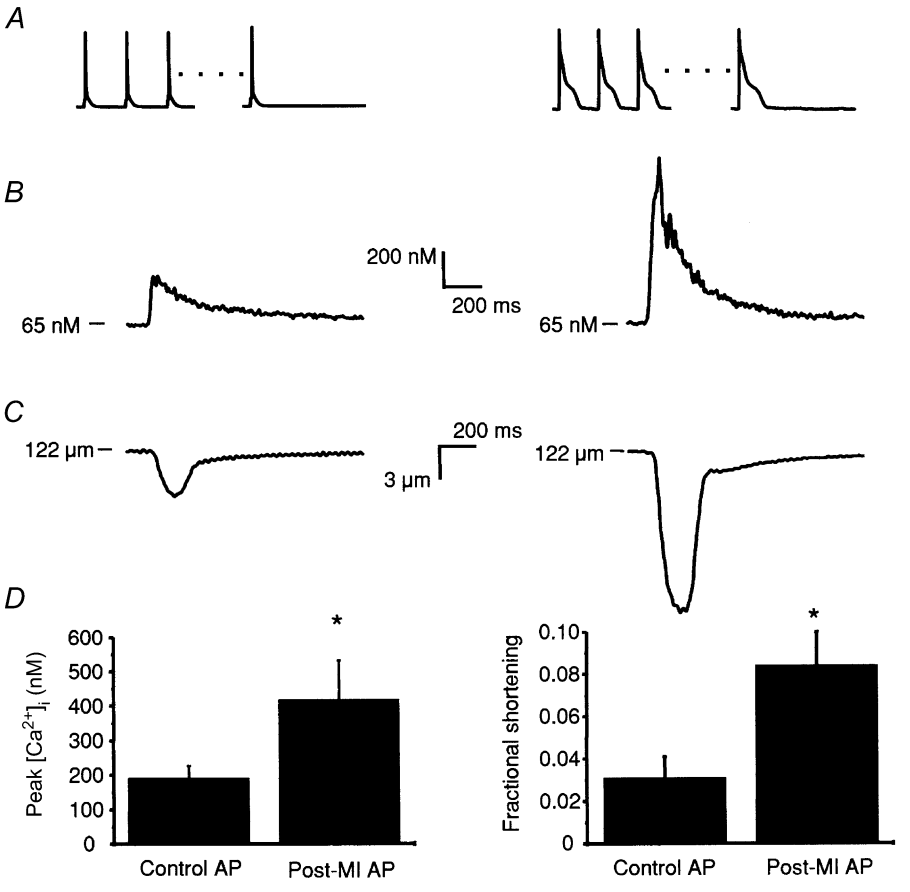


**Figure 1. Prolonged action potentials increase $Ca^{2+}$ transients and unloaded cell shortening in rat cardiac myocytes**

*A*, trains of eight short control APs (left) and long post-MI APs (right) were used to load the myocyte to steady-state SR $Ca^{2+}$ load. *B*, $Ca^{2+}$ transients measured from the final 9th control AP (left panel) and post-MI AP (right panel). *C*, unloaded cell shortening associated with the intracellular $Ca^{2+}$ transient and triggered by the control AP (left) and post-MI AP (right). *D*, peak intracellular $[Ca^{2+}]$ (left) is elevated 2.2-fold upon stimulation with a post-MI AP relative to the control AP while fractional cell shortening (right) is increased 2.7-fold. * $P < 0.05$.

stimulation with test APs were significantly elevated from 190 ± 37 nM ($n = 5$) with short control APs to 417 ± 115 nM ($n = 5$) with long post-MI APs, without affecting the resting diastolic levels. Associated with elevated $Ca^{2+}$ transients there was a 2.7-fold increase in peak fractional cell shortening ($P < 0.05$) triggered by a long post-MI AP (0.084 ± 0.016, $n = 7$) compared with a short control AP (0.031 ± 0.010, $n = 7$), shown in Fig. 1*C* and *D* (right). These results establish that AP prolongation, as occurs with a reduction in $I_{to}$ following myocardial infarction, can significantly enhance contractility of the surviving myocytes.

The mechanism responsible for increased peak systolic $Ca^{2+}$ transients and peak cell shortening following AP prolongation may arise from enhanced SR $Ca^{2+}$ loading, enhanced triggered SR $Ca^{2+}$ release, or both. To examine the contribution of SR $Ca^{2+}$ load to these measured changes in $[Ca^{2+}]_i$ we recorded the inward $Na^+$–$Ca^{2+}$ exchange current at −80 mV in response to a rapid application of 20 mM caffeine to the cell, and converted the integrated current into SR $Ca^{2+}$ content (Varro *et al.* 1993), using a correction factor of 0.87 to account for $Ca^{2+}$ extrusion via non-electrogenic means (Bassani *et al.* 1994). As shown in Fig. 2, the SR $Ca^{2+}$ content after a train of short control APs (56 ± 7.2 μmol $l^{-1}$, $n = 7$) was reduced ($P < 0.05$) to about half of that measured with long post-MI APs (111 ± 21.6 μmol $l^{-1}$, $n = 4$) similar to previous studies (Terracciano *et al.* 1997).

### SR $Ca^{2+}$ release triggered by control and post-MI APs at equal, low and high SR $Ca^{2+}$ loads

To address whether the positive inotropic effect of post-MI APs acts via increases in SR $Ca^{2+}$ load or enhanced triggered $Ca^{2+}$ release, we applied control and post-MI APs to normal myocytes loaded to a fixed steady-state level of SR $Ca^{2+}$ using a train of eight 100 ms depolarizing steps to +10 mV (Fig. 3*A*) (Trafford *et al.* 1997). Typical intracellular $Ca^{2+}$ transients and fractional cell shortening are shown in Fig. 3*B* and *C*, respectively, while Fig. 3*D* summarizes the $Ca^{2+}$ transients and cell shortening from seven to nine cells. On average $Ca^{2+}$ transients were significantly elevated 1.7-fold ($P < 0.005$) from 242 ± 22 to 404 ± 46 nM while fractional cell shortening increased 3.8-fold ($P < 0.05$) from 0.014 ± 0.004 to 0.053 ± 0.015. Thus, under conditions of equal SR $Ca^{2+}$ load, post-MI AP waveforms alone are capable of triggering significantly more $Ca^{2+}$ release and evoking a larger degree of cell shortening than control AP waveforms. A comparison of the data in Figs 1 and 3 further reveals that both peak $Ca^{2+}$ transients and cell shortening triggered by either control or post-MI APs were similar whether myocytes were loaded to different extents with different APs or to the same extent using 100 ms steps. This suggests that changes in the triggering of $Ca^{2+}$ release, rather than SR load, play a dominant role in mediating enhancements in SR $Ca^{2+}$ release following AP prolongation under our experimental conditions.

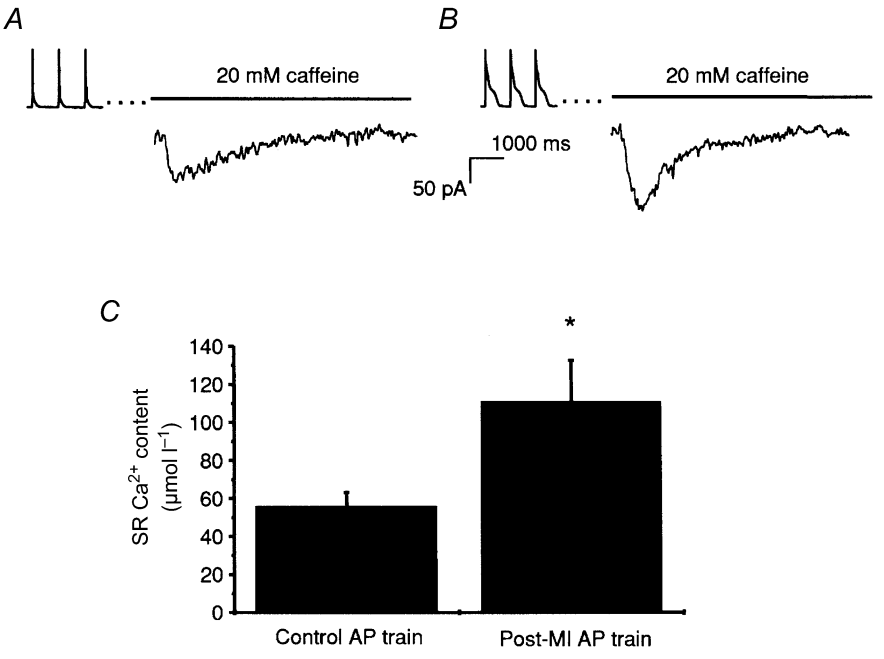


**Figure 2. SR $Ca^{2+}$ load after conditioning trains of short control and long post-MI action potentials**

Representative current traces of inward $Na^+$–$Ca^{2+}$ exchange current during a 20 mM caffeine spritz after a train of short control APs (*A*) and long post-MI APs (*B*). *C*, SR $Ca^{2+}$ content calculated from the integrated $Na^+$–$Ca^{2+}$ exchange current after loading trains of control APs (56 ± 7.2 μmol $l^{-1}$, $n = 7$) and post-MI APs (111 ± 21.6 μmol $l^{-1}$, $n = 4$). * $P < 0.05$.

Next we investigated the possible contributions of SR load in mediating changes in $Ca^{2+}$ release and cell shortening. Figure 4 shows that, following loading with eight short APs (i.e. low SR load), a post-MI AP triggered significantly ($P < 0.05$) more $Ca^{2+}$ release (314 ± 64 nM, $n = 7$) than a control AP (198 ± 28 nM, $n = 7$) preceded by eight long post-MI APs (i.e. high SR load). Furthermore, fractional cell shortening was also significantly enhanced ($P < 0.05$) under these conditions ($CS_{control} = 0.042 \pm 0.010$; $CS_{post\text{-}MI} = 0.076 \pm 0.016$, $n = 7$). Remarkably, the $Ca^{2+}$ released by a post-MI AP with a low SR load produced a 1.6-fold increase in peak $[Ca^{2+}]_i$ transient relative to control APs with a high SR load (Fig. 4*D*). By comparison, post-MI APs caused a 2.2-fold increase compared with control APs under the opposite loading conditions (Fig. 1). Thus, while the positive inotropic effects of AP prolongation appears to be dominated by enhancements in triggered SR $Ca^{2+}$ release, a measurable, yet small, contribution of SR $Ca^{2+}$ load to $Ca^{2+}$ release also exists under our experimental conditions.

To further quantify the relative contributions of trigger and SR $Ca^{2+}$ load to the amount of $Ca^{2+}$ released from the SR following changes in AP profile, we calculated $\Delta[Ca^{2+}]$ ($[Ca^{2+}]_{systolic} - [Ca^{2+}]_{diastolic}$) since this should provide a better measure of the changes in $[Ca^{2+}]_i$ resulting from SR $Ca^{2+}$ release than does peak $[Ca^{2+}]_i$ (Han *et al.* 1994; Isenberg & Han, 1994; Janczewski *et al.* 1995; Santana *et al.* 1997). To eliminate inter-cell variability in this analysis, the $\Delta[Ca^{2+}]_i$ released for each protocol was normalized by the response measured during a control AP following loading with a train of control APs. As shown in Fig. 5, the $Ca^{2+}$ released at either low or high SR loads increased ~2-fold when short control APs were replaced with long post-MI APs as expected if the trigger for $Ca^{2+}$ release is the dominant determinant of release. This is similar to the 1.7-fold enhancement in $Ca^{2+}$ release shown

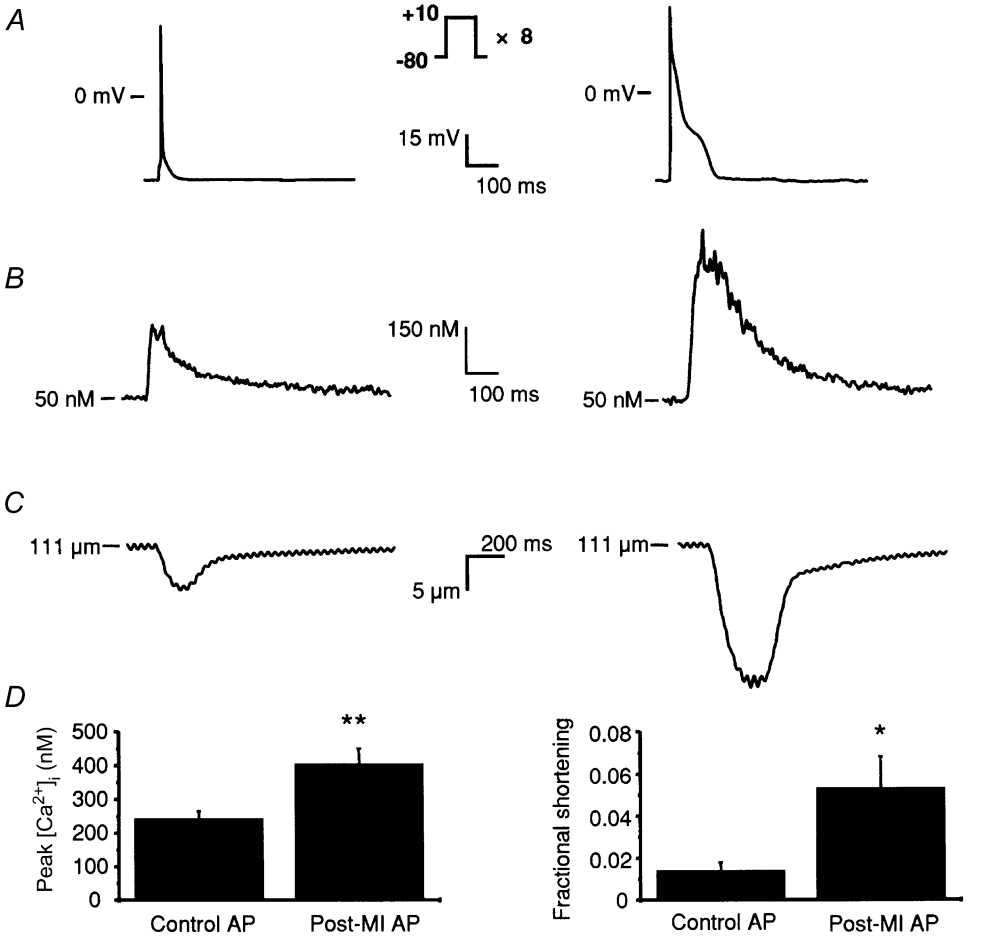


**Figure 3. Calcium transients and cell shortening triggered by action potentials under conditions of equal SR load**

*A*, the voltage protocols: control and post-MI APs were applied to myocytes after a loading protocol of eight 100 ms steps to +10 mV. *B*, representative $Ca^{2+}$ transients triggered by the control AP (left) and post-MI AP (right). *C*, fractional cell shortening associated with the intracellular $Ca^{2+}$ transients triggered by control (left) and post-MI (right) APs. *D*, peak $Ca^{2+}$ transients (left) are elevated 1.7-fold upon stimulation with a post-MI AP relative to the control AP while fractional cell shortening (right) is increased 3.8-fold. * $P < 0.05$; ** $P < 0.005$.

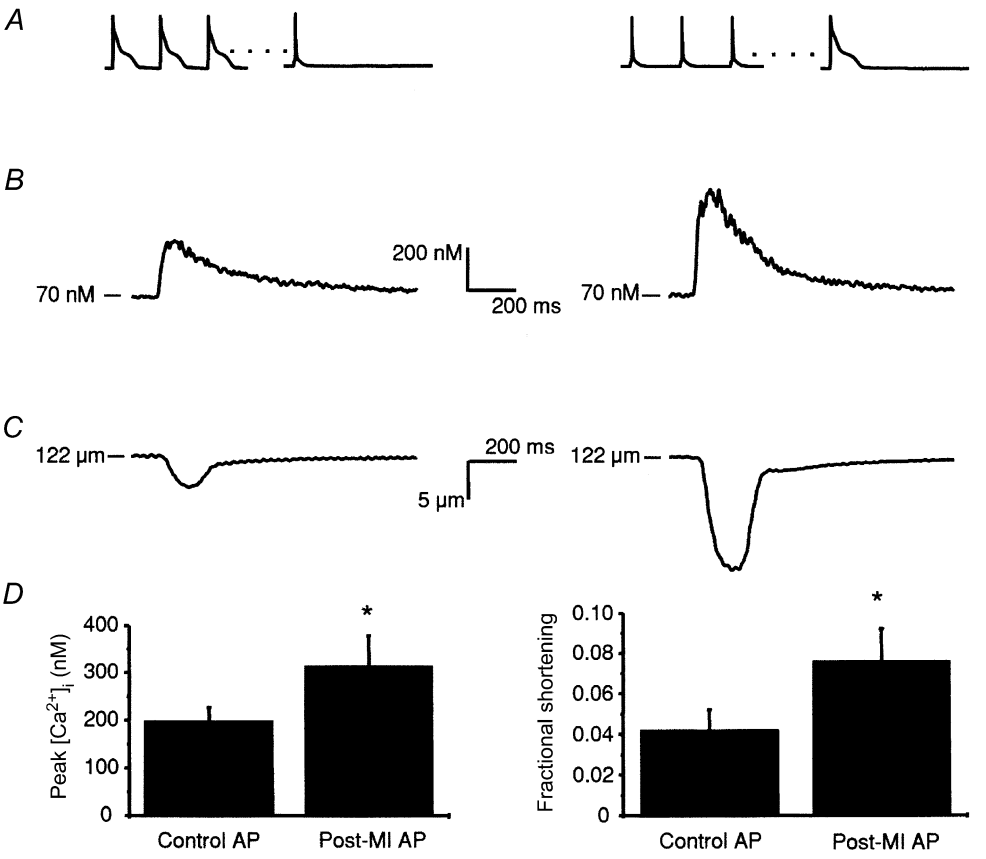


**Figure 4. Effect of high and low SR load on $Ca^{2+}$ transients and cell shortening triggered by action potentials**

*A*, the voltage protocols: trains of eight post-MI APs (left) or control APs (right) were used to achieve a high or low steady-state SR load. $Ca^{2+}$ release was then triggered from the SR with either a control AP (left) or post-MI AP (right). *B*, representative intracellular $Ca^{2+}$ transients triggered by the high SR load/control AP protocol (left) and low SR load/post-MI AP protocol (right). *C*, typical fractional cell shortening associated with the $Ca^{2+}$ transients shown in *B*. *D*, peak $Ca^{2+}$ transients (left) triggered by post-MI APs under conditions of low SR load are increased 1.6-fold over transients triggered by control APs at a high SR load, while fractional shortening measurements (right) show a 1.8-fold difference between low SR load/post-MI AP and high SR load/control AP protocols. $*P < 0.05$.

in Fig. 3 between control and post-MI APs under equal SR $Ca^{2+}$ load conditions. On the other hand, the relative increase in $Ca^{2+}$ release due to changes in SR load from low to high was found to be only 1.2-fold when triggered with either a short control or long post-MI AP. Collectively, these data strongly suggest that changes in SR $Ca^{2+}$ load account for at most about 20% of the differences in contractility observed following AP prolongation.

## Efficiency of SR $Ca^{2+}$ release by control and post-MI APs

Having demonstrated that alterations in the AP waveform are capable of enhancing SR $Ca^{2+}$ release, the question remains whether this arises exclusively from changes in $I_{Ca,L}$ or whether there are also changes in the *efficiency* of $Ca^{2+}$ release by $I_{Ca,L}$. To quantify the efficiency

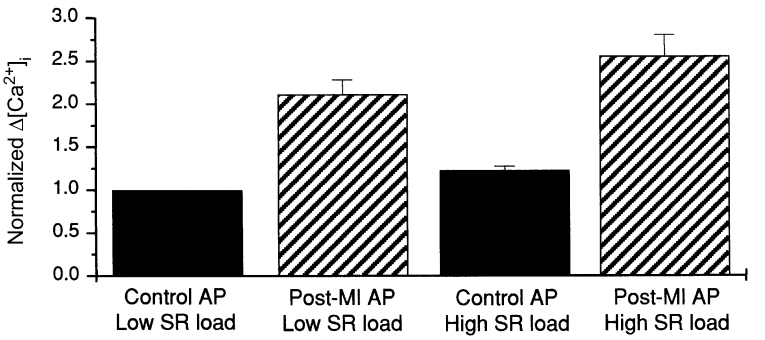


**Figure 5. Effect of control and post-MI action potentials on $Ca^{2+}$ release at low and high SR $Ca^{2+}$ loads**

Relative $Ca^{2+}$ release triggered by control and post-MI APs at low (control AP train) and high (post-MI AP train) SR loads. Data are normalized to the amplitude of $\Delta[Ca^{2+}]_i$ triggered by the control AP at a low SR load.

**Table 1. Parameters describing L-type $Ca^{2+}$ flux and SR $Ca^{2+}$ release during control and post-MI APs**

| AP | $I_{Ca,L}$ (pA pF$^{-1}$) | $Q_{Ca,L}$ (pC) | $2\int_o^{peak} I_{Ca,L}dt$ (pC) | $\int F_{Ca,L}$ ($\mu$M) | $\int F_{rel}$ ($\mu$M) | d(CS)/d$t$ ($\mu$m s$^{-1}$) |
|---|---|---|---|---|---|---|
| Control AP | 13.5 ± 1.9 | 8.2 ± 1.4 | 7.7 ± 1.4 | 0.39 ± 0.07 | 31.7 ± 4.5 | 33 ± 9.4 |
| Post-MI AP | 6.2 ± 1.4* | 23.8 ± 4.3* | 14.1 ± 2.9* | 0.71 ± 0.15* | 70.9 ± 8.4* | 88.8 ± 20* |

Calcium influx and SR $Ca^{2+}$ release were triggered by AP clamps after loading with eight 100 ms square waves as shown in Figs 6 and 7. $I_{Ca,L}$, peak $Ca^{2+}$ current; $Q_{Ca,L}$, total charge influx obtained by integrating the L-type $Ca^{2+}$ current trace ($n = 5$); $2\int_o^{peak} I_{Ca,L}dt$ indicates the charge influx reflecting the first latency of $Ca^{2+}$ channel openings ($n = 5$); $\int F_{Ca,L}$, the integrated trans-sarcolemmal $Ca^{2+}$ flux derived from $2\int_o^{peak} I_{Ca,L}dt$ ($n = 5$); $\int F_{rel}$, the integrated SR $Ca^{2+}$ release flux ($n = 9$); d(CS)/d$t$, the rate of cell shortening ($n = 8$). Both $\int F_{Ca,L}$ and $\int F_{rel}$ are $Ca^{2+}$ concentrations in the $Ca^{2+}$-accessible cell volume or half the total cell volume (Sipido & Wier, 1991). * $P < 0$ 05.

of SR $Ca^{2+}$ release, $I_{Ca,L}$ was measured simultaneously with $Ca^{2+}$ transients. L-type $Ca^{2+}$ current was recorded by a near complete replacement of intracellular $K^+$ with $Cs^+$ to eliminate interfering potassium currents and superfusion of the myocytes with extracellular solution containing 30 $\mu$M TTX to eliminate $Na^+$ currents. The records in Fig. 6 show the $Cd^{2+}$-sensitive L-type $Ca^{2+}$ currents and associated intracellular $Ca^{2+}$ transients produced by short control (left) and long post-MI APs (right) after loading with eight 100 ms steps. The amplitude and time course of $Ca^{2+}$ influx driven by control and post-MI APs were remarkably different (Fig. 6*B*, left and right, respectively) and their characteristics are summarized in Table 1. Despite an ~2-fold reduction in

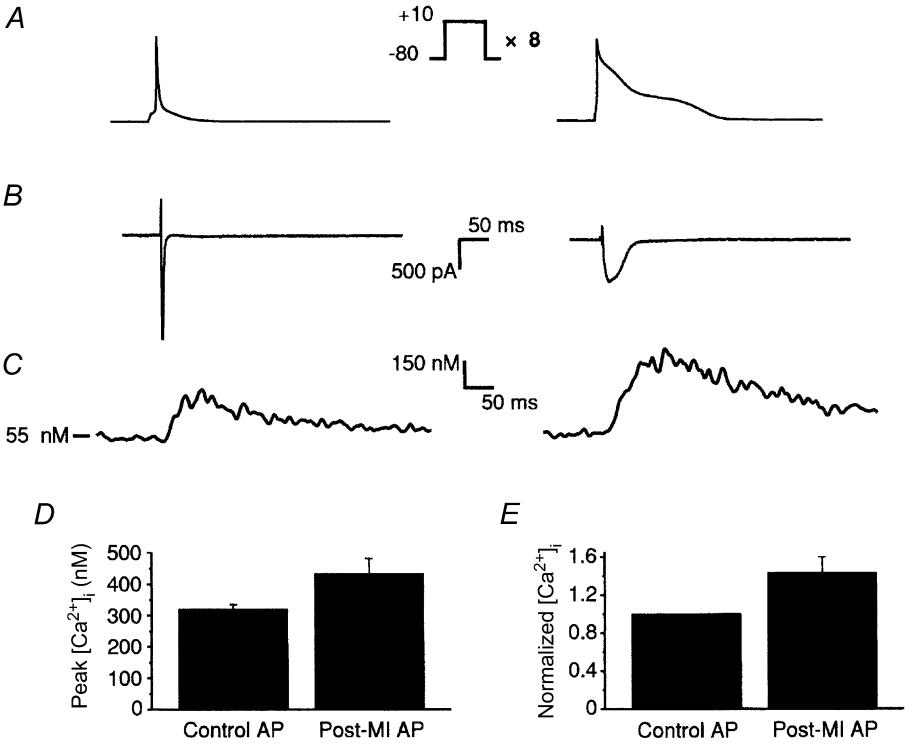


**Figure 6. L-type $Ca^{2+}$ currents and $Ca^{2+}$ transients evoked by short control and long post-MI action potentials**

*A*, the voltage protocols: control (left) and post-MI (right) APs were applied to $Cs^+$-loaded rat ventricular myocytes following a loading train of eight 100 ms steps to +10 mV. *B*, $Ca^{2+}$ currents evoked by the control and post-MI APs were measured as $Cd^{2+}$-sensitive currents and differed in peak amplitude, time to peak and integrated current. Table 1 summarizes the characteristics of $I_{Ca,L}$ during control and post-MI APs. *C*, representative intracellular $Ca^{2+}$ transients triggered by control and post-MI APs. *D*, peak systolic $Ca^{2+}$ was not significantly different between control (319.2 ± 16.1 nM, $n = 5$) and post-MI APs (433.4 ± 48.2 nM, $n = 5$). *E*, normalized peak $Ca^{2+}$ transients of the post-MI AP were only 1.4-fold greater than the control AP under these intracellular conditions.

peak $I_{Ca,L}$ ($P < 0.001$) with the post-MI AP relative to the control AP ($I_{Ca,L,control} = 13.5 \pm 1.9$ pA pF$^{-1}$, $I_{Ca,L,post\text{-}MI} = 6.2 \pm 1.4$ pA pF$^{-1}$, $n = 5$), the total integrated $I_{Ca,L}$ ($Q_{control} = 8.2 \pm 1.4$ pC, $Q_{post\text{-}MI} = 23.8 \pm 4.3$ pC, $n = 5$) was actually increased about 3-fold ($P < 0.01$).

As expected from the differences in integrated $I_{Ca,L}$, Fig. 6*C* and *D* further establishes that peak $Ca^{2+}$ transients were elevated following stimulation with post-MI relative to control APs, although the effect was less pronounced, possibly due to the replacement of $K^+$ with $Cs^+$, which impairs SR $Ca^{2+}$ release (Levi *et al.* 1996; Wasserstrom & Vites, 1996; Litwin *et al.* 1998) (see Discussion). On the other hand, $Ca^{2+}$ channel gating has previously been shown to be largely unaffected by high intracellular [$Cs^+$] (Levi *et al.* 1996). Therefore, in an attempt to obtain the best estimate of the true E–C coupling gain, we decided to combine the $I_{Ca,L}$ recordings from the $Cs^+$ studies with the $Ca^{2+}$ transient and cell shortening data recorded using high $K^+$ pipette solutions (Isenberg & Han, 1994) (shown previously in Fig. 3), although similar results were observed when $Ca^{2+}$ transients are recorded in the presence of $Cs^+$ (see Discussion).

Excitation–contraction coupling gains provide estimates of the effectiveness of $Ca^{2+}$ release in response to the $I_{Ca,L}$ trigger and have been calculated previously in a number of different ways (Wier *et al.* 1994; Janczewski *et al.* 1995; Santana *et al.* 1997; Litwin *et al.* 1998). We used two different definitions (see Methods for rationale and details): E–C gain$_1$ $= \int F_{rel} / \int F_{Ca,L}$ and E–C gain$_2$ $= \mathrm{d(CS)}/\mathrm{d}t / \int F_{Ca,L}$. As stated in Methods, our definitions required integration of the $F_{rel}$ and $F_{Ca,L}$ since the kinetic properties of $I_{Ca,L}$ are strongly influenced by the AP profile. Typical SR release fluxes, $F_{rel}$, triggered by long post-MI and short control APs are shown in Fig. 7*C*, right and left, respectively, with their associated intracellular

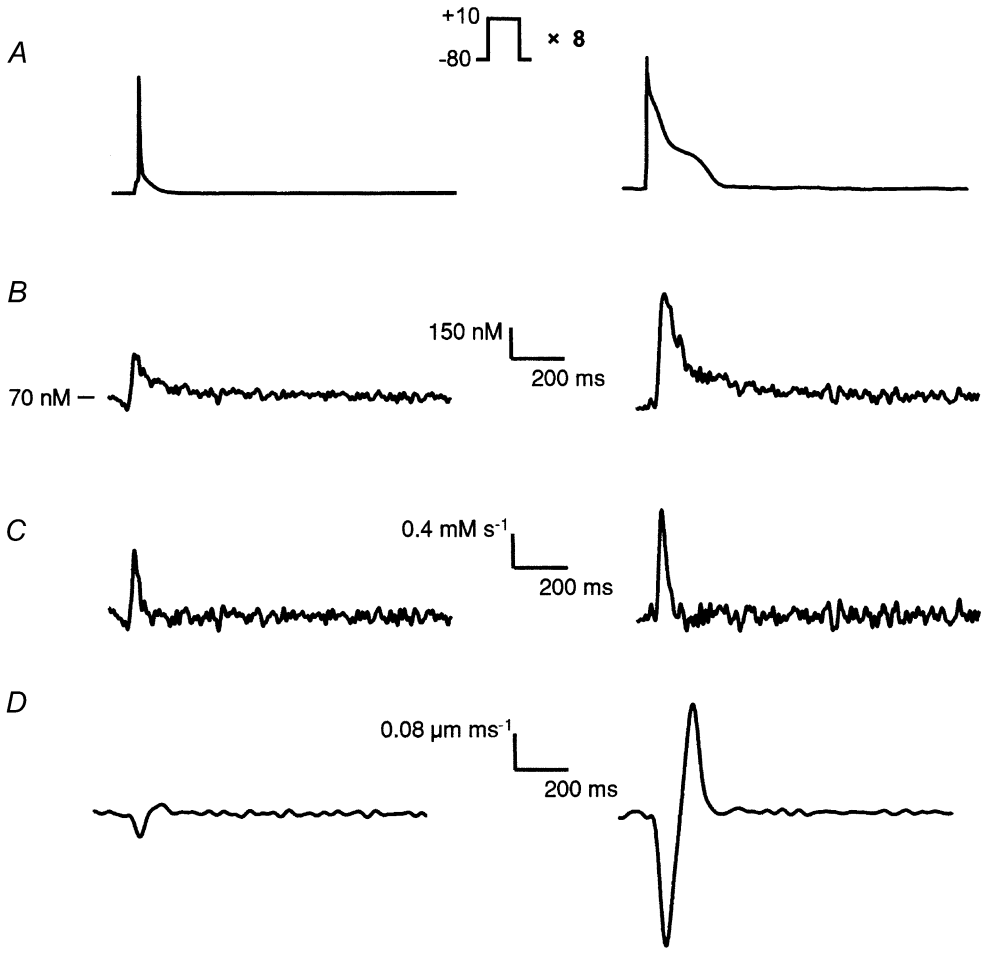


**Figure 7. Parameters reflecting $Ca^{2+}$ release in isolated rat ventricular myocytes**

*A*, control (left) and post-MI (right) APs were applied to myocytes after a loading protocol of eight 100 ms steps to +10 mV. *B*, kinetically corrected intracellular $Ca^{2+}$ transients triggered by control and post-MI APs. These data were used to calculate the SR release flux, $F_{rel}$, according to the equation: $\mathrm{d}[Ca^{2+}]_i/\mathrm{d}t = F_{rel} + F_{pump} + F_{leak} + \sum \mathrm{d[CaL]}/\mathrm{d}t$ (see Methods). *C*, SR release flux, $F_{rel}$, triggered by short control and long post-MI APs. *D*, rate of unloaded cell shortening, d(CS)/d$t$, triggered by control and post-MI APs.

$Ca^{2+}$ transients plotted in Fig. 7*B*. Figure 7*D* shows the corresponding rates of cell shortening. For the purposes of calculating E–C coupling gain, the integrated SR $Ca^{2+}$ flux ($\int F_{rel}$, see Table 1), was used to provide an estimate of the total $Ca^{2+}$ released from the SR. Using the first definition of E–C coupling gain, the efficiency of $Ca^{2+}$ release by $I_{Ca,L}$ during a long post-MI AP was elevated about 1.2-fold ($P < 0.05$) over the control AP (Fig. 8*A*). Similarly, the second definition of gain indicated a 1.5-fold ($P < 0.05$) enhancement in SR $Ca^{2+}$ release efficiency by the long post-MI AP as compared with the short control AP (Fig. 8*B*). The calcium release from the SR was also quantified by calculating the fractional SR $Ca^{2+}$ release by post-MI and control APs following 100 ms loading steps. The total SR content under these conditions was measured as $148 \pm 15$ $\mu$mol $l^{-1}$ and the fraction of SR $Ca^{2+}$ released (FR) by the post-MI AP ($24 \pm 3$ %, $n = 9$) was found to be elevated compared with the control AP ($11 \pm 2$ %, $n = 9$) (Fig. 8*C*). Normalizing the FR to the integrated L-type $Ca^{2+}$ flux (FR/$\int F_{Ca,L}$; Fig. 8*D*) revealed a 1.2-fold relative increase between control and post-MI APs. These results suggest that AP prolongation not only enhances triggered $Ca^{2+}$ release by producing a more powerful $Ca^{2+}$ influx trigger, but also modestly increases the efficiency of SR $Ca^{2+}$ release by $I_{Ca,L}$.

## DISCUSSION

Changes in AP morphology and duration occur with heart disease in humans as well as in numerous animal models and are typically associated with reductions in transient outward currents (Beuckelmann *et al.* 1993; Coulombe *et al.* 1994; Wettwer *et al.* 1994; Potreau *et al.* 1995; Kaab *et al.* 1996; Wickenden *et al.* 1998; Kaprielian *et al.* 1999). We have shown previously that following myocardial infarction $Ca^{2+}$ transient amplitudes are increased as a result of AP prolongation (Kaprielian *et al.* 1999). In this study, we extended this work by examining the possible mechanisms responsible for these observations.

Measurements of caffeine-induced $Na^+$–$Ca^{2+}$ exchange current revealed a doubling of the steady-state SR $Ca^{2+}$ content in myocytes stimulated with post-MI APs *versus* control APs. However, changes in SR load only accounted for a fraction of the increased $Ca^{2+}$ transient amplitude associated with AP prolongation characteristically observed in diseased myocardium (Kaprielian *et al.* 1999). Specifically, $\Delta[Ca^{2+}]_i$ was only increased by about 20 % when the SR load was elevated by loading with long post-MI APs whether the trigger for $Ca^{2+}$ release was a short control or long post-MI AP. By contrast, with equal SR $Ca^{2+}$ loads, the increase in $Ca^{2+}$ release triggered by the post-MI AP was consistently found to be about 2-fold

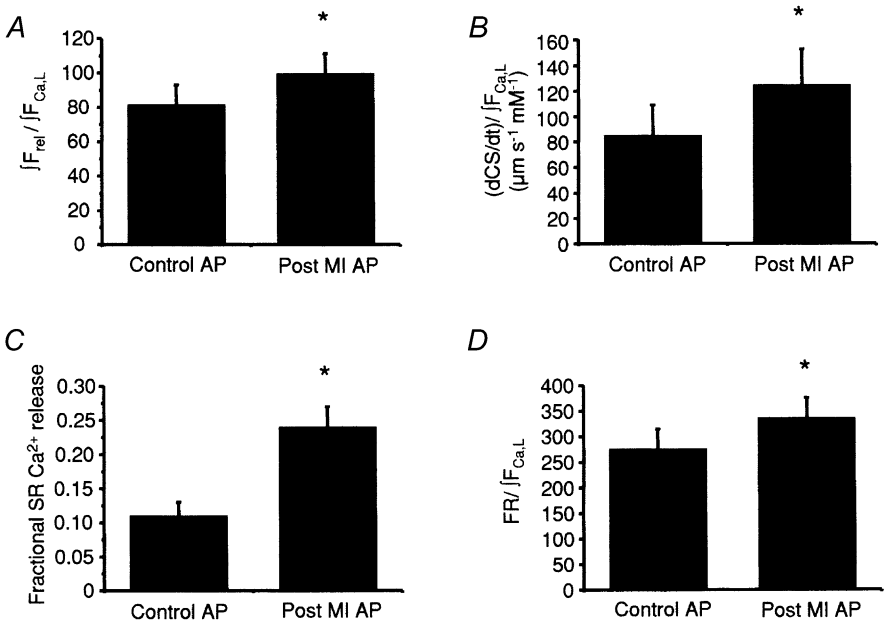


**Figure 8. Excitation–contraction coupling gains and fractional SR $Ca^{2+}$ release during short control and long post-MI action potentials**

*A*, a 1.2-fold enhancement in E–C coupling gain in myocytes stimulated with a long post-MI AP ($99.6 \pm 11.7$, $n = 9$) relative to a short control AP ($81.6 \pm 11.5$, $n = 9$) when gain is defined as the estimated amount of SR $Ca^{2+}$ release ($\int F_{rel}$) over the amount of trigger $Ca^{2+}$ ($\int F_{Ca,L}$). *B*, the E–C coupling gain as defined by the rate of cell shortening over the amount of trigger $Ca^{2+}$. According to this definition, E–C coupling efficiency is elevated 1.5-fold upon stimulation of myocytes with a long post-MI AP ($124.6 \pm 28.2$ $\mu$m $s^{-1}$ $mM^{-1}$, $n = 8$) relative to a short control AP ($84.8 \pm 24.2$ $\mu$m $s^{-1}$ $mM^{-1}$, $n = 8$). *C*, fractional release (FR) is enhanced by the post-MI AP ($24 \pm 3$ %, $n = 9$) over the control AP ($11 \pm 2$ %, $n = 9$) and the FR normalized to the amount of trigger $Ca^{2+}$ ($\int F_{Ca,L}$) was increased 1.2-fold (*D*). * $P < 0.05$.

larger than the control AP trigger regardless of the loading protocol. This relationship between $Ca^{2+}$ release, SR load and AP trigger suggests that the effects of SR load on $Ca^{2+}$ release, under the experimental conditions used in the present study (high intracellular $K^+$, 23 °C), are small relative to the effects of the AP profile in triggering release. At first glance these findings appear to contradict a previous report concluding that the positive inotropic effects following AP prolongation result from increased SR $Ca^{2+}$ loading (Bouchard *et al.* 1995). This discrepancy might be readily explained by differences in the experimental conditions. In our study, we compared the effects of long and short APs obtained from post-MI and control myocytes, which may be very different from studies using high doses of 4-aminopyridine (4-AP) to prolong APs. In addition, our experiments were conducted using high intracellular $K^+$ solutions while those of Bouchard *et al.* (1995) used $Cs^+$ to replace $K^+$. Previous reports have consistently shown significant changes in E–C coupling when $K^+$-based intracellular solutions are replaced with $Cs^+$ (Levi *et al.* 1996; Wasserstrom & Vites, 1996; Litwin & Bridge, 1997), apparently as a result of the inhibitory action of $Cs^+$ on both SR $Ca^{2+}$ release (Litwin & Bridge, 1997) and the contribution of the $Na^+$–$Ca^{2+}$ exchanger to the $Ca^{2+}$ release process (Levi *et al.* 1996; Wasserstrom & Vites, 1996). In concordance with these studies we found that the enhancement of peak $[Ca^{2+}]_i$ by long post-MI APs relative to short control APs was reduced from 1.7-fold in the presence of high $K^+$ to only 1.4-fold in the presence of $Cs^+$. Regardless, recording in the presence of intracellular $K^+$ is unquestionably more physiologically relevant when studying the mechanism by which changes in AP profile affect intracellular $Ca^{2+}$ and inotropy in disease (Isenberg & Han, 1994; Levi *et al.* 1996; Wasserstrom & Vites, 1996).

It is clear that reductions in $I_{to}$ and resultant prolongation of the rat cardiac AP cause increased $Ca^{2+}$ release from the SR, independent of the SR $Ca^{2+}$ load. It seems reasonable to postulate that the differences in the release of $Ca^{2+}$ between long post-MI and short control APs are a consequence, at least in part, of differences in $Ca^{2+}$ influx 'trigger' (Fig. 6*B*) (Bassani *et al.* 1995; Lopez-Lopez *et al.* 1995; Santana *et al.* 1996). The $Ca^{2+}$ current from the control AP has a large amplitude but a very short duration compared with post-MI APs, which probably reflects the relative differences in the rate of deactivation, associated with repolarization, *versus* inactivation of $I_{Ca,L}$ (Kaprielian *et al.* 1999). The effects of $I_{to}$ on the trajectory of early repolarization of the AP and its close temporal association with $Ca^{2+}$ channel gating may account for the ability of changes in $I_{to}$ to so profoundly modulate $Ca^{2+}$ influx. Indeed, $Ca^{2+}$ release depends steeply on the early portion of the pulse stimulus between 0 and 20 ms, and not on pulses of longer duration (Han *et al.* 1994; Isenberg & Han, 1994; P. H. Backx & R. Kaprielian, unpublished observations). The differences in integrated L-type $Ca^{2+}$ current between control and post-MI APs may reflect changes in the degree of activation of $I_{Ca,L}$. Since the upstroke velocities and peaks of control and post-MI APs are quite similar, the enhanced activation of $I_{Ca,L}$ by the post-MI AP could result from a slower repolarization rate, thereby allowing more time for $Ca^{2+}$ channel activation. Therefore, the enhanced $Ca^{2+}$ release triggered by post-MI APs may result from the recruitment of more $Ca^{2+}$ release units by a larger, more sustained L-type $Ca^{2+}$ influx. On the other hand, the large but short-lived L-type $Ca^{2+}$ flux occurring during short control APs may reflect the transient opening of smaller numbers of $Ca^{2+}$ channels and thus activate fewer $Ca^{2+}$ release units.

To assess whether the enhanced $Ca^{2+}$ transient amplitudes could be attributed exclusively to larger $Ca^{2+}$ triggers or whether changes in the efficiency of $Ca^{2+}$ release also occur when myocytes are stimulated with a post-MI AP, we calculated the E–C coupling gain. We formulated two definitions of E–C coupling gain, (1) $\int F_{rel}/\int F_{Ca,L}$ and (2) $d(CS)/dt/\int F_{Ca,L}$, based in part on previous reports (Wier *et al.* 1994; Janczewski *et al.* 1995; Santana *et al.* 1997; Litwin *et al.* 1998). Both definitions of E–C coupling gain predicted that the efficiency of $Ca^{2+}$ release increased modestly in comparison to enhancements in either cell shortening or $Ca^{2+}$ transient amplitude when stimulated with long post-MI APs *versus* short control APs. These findings suggest that it is the increase in trigger $Ca^{2+}$ through L-type $Ca^{2+}$ channels that is primarily responsible for the enhancement in contractility observed with AP prolongation.

Interestingly, the relative increase in E–C coupling gain was larger when cell shortening rate (Fig. 8*B*) rather than SR $Ca^{2+}$ release (Fig. 8*A*) was used as a measure of E–C coupling. This finding is consistent with the existence of an inherent amplification factor between intracellular $Ca^{2+}$ and activation of contractile proteins due to the very steep relationship between contractile force and $[Ca^{2+}]_i$ arising from the positive cooperativity of $Ca^{2+}$ binding to troponin C (Backx *et al.* 1995). These results suggest that a distinction should generally be made between *contraction* and *release* following myocyte excitation. Alternatively, the difference in gains as assessed by $Ca^{2+}$ release *versus* cell shortening may also arise from the absence of $Na^+$–$Ca^{2+}$ exchange current, $I_{Na-Ca}$, in the equation describing $F_{rel}$. Under our experimental conditions $Na^+$–$Ca^{2+}$ exchange is present but was not included in the estimation of $F_{rel}$. Calcium efflux through the exchanger will result in an underestimation of $F_{rel}$ and this efflux is expected to be greater with long post-MI APs since peak intracellular $Ca^{2+}$ levels are higher.

The mechanism by which a prolonged post-MI AP increases the efficiency of $Ca^{2+}$ release is unclear. One possible explanation may be enhancements of reverse-mode $Na^+$–$Ca^{2+}$ exchange since the magnitude and time course of reverse-mode $Na^+$–$Ca^{2+}$ exchange depend strongly on the profile of the AP during this time period

(Bers, 1992). This possibility is supported by recent studies showing that reverse mode $Na^+$–$Ca^{2+}$ exchange activity works synergistically with $I_{Ca,L}$ in triggering $Ca^{2+}$ release from the SR (Litwin *et al.* 1998; Cordeiro *et al.* 2000; Piacentino & Houser, 2000). Studies are currently underway in our laboratory to determine the potential role of the $Na^+$–$Ca^{2+}$ exchanger in modulating $Ca^{2+}$ release following changes in action potential profile.

In this study the effects of AP prolongation on E–C coupling following infarction were examined by comparing $Ca^{2+}$ release in healthy rat ventricular myocytes stimulated with APs previously recorded from control and post-MI rat myocytes. The similarity of the changes in intracellular $Ca^{2+}$ measured following AP prolongation in normal myocytes *versus* post-infarction myocytes substantiates further our previous conclusion that elevated $Ca^{2+}$ transients following infarction are due primarily to AP prolongation (Kaprielian *et al.* 1999). However, numerous other genetic, biochemical and morphological changes, aside from $I_{to}$ downregulation, can affect intracellular $Ca^{2+}$ handling, E–C coupling and AP profile in heart disease (Gwathmey *et al.* 1987; Beuckelmann *et al.* 1992; Arai *et al.* 1993; Gomez *et al.* 1997; Litwin & Bridge, 1997; Balke & Shorofsky, 1998; O'Rourke *et al.* 1999; Shorofsky *et al.* 1999). Therefore, the effect of AP prolongation on E–C coupling shown in our studies may be modulated by other changes affecting $Ca^{2+}$ handling in diseased myocytes. Nevertheless, our results show that AP profile-mediated alterations in E–C coupling can significantly influence $Ca^{2+}$ handling in heart disease independent of these other possible contributing effects.

Recently, Shorofsky *et al.* (1999) and Gomez *et al.* (1997) published contradictory results regarding changes in E–C coupling in the spontaneous hypertensive rat (SHR). Both studies used square wave voltage clamp waveforms to trigger $Ca^{2+}$ release and thereby ignored the possible influences of AP profile on E–C coupling. Indeed, SHRs have prolonged APs (Brooksby *et al.* 1993; Cerbai *et al.* 1994), reductions in $I_{to}$ (Cerbai *et al.* 1994) and elevated $Ca^{2+}$ transients similar to those seen following myocardial infarction (Kaprielian *et al.* 1999). Based on our findings, AP prolongation in other heart disease models should be considered when drawing conclusions about changes in E–C coupling within the context of disease.

Although we studied the effects of AP prolongation following myocardial infarction on E–C coupling in the rat, similar changes in AP profile may also affect E–C coupling in failing human myocytes. Human epicardial myocytes have been shown to have a relatively high transient outward current density, which is believed to be responsible for their short, notched APs (Nabauer *et al.* 1996). In human heart failure, a reduction in $I_{to}$ is associated with a slowed rate of early repolarization and a loss of the AP notch (Beuckelmann *et al.* 1993; Kaab *et al.* 1996). Based on our findings, changes in the profile of the human AP as occur in heart failure could conceivably also affect trigger $I_{Ca,L}$ and E–C coupling efficiency thereby influencing contractility in a manner similar to what we have found in rat.

In summary, our results establish that the positive inotropic effects of prolonged APs as observed following myocardial infarction in rat are mediated primarily through increases in triggered $Ca^{2+}$ release rather than enhanced SR loads. This increase in $Ca^{2+}$ release is due to stronger trigger $Ca^{2+}$ influxes through L-type $Ca^{2+}$ channels coupled with modest enhancements of $Ca^{2+}$ release efficiency. The effect of $I_{to}$ on excitation–contraction coupling via alterations in AP morphology may represent an important compensatory process by which the myocardium increases contractility following an infarction.

Arai, M., Alpert, N. R., MacLennan, D. H., Barton, P. & Periasamy, M. (1993). Alterations in sarcoplasmic reticulum gene expression in human heart failure. A possible mechanism for alterations in systolic and diastolic properties of the failing myocardium. *Circulation Research* **72**, 463–469.

Backx, P. H., Gao, W. D., Azan-Backx, M. D. & Marban, E. (1995). The relationship between contractile force and intracellular [$Ca^{2+}$] in intact rat cardiac trabeculae. *Journal of General Physiology* **105**, 1–19.

Balke, C. W., Egan, T. M. & Wier, W. G. (1994). Processes that remove calcium from the cytoplasm during excitation–contraction coupling in intact rat heart cells. *Journal of Physiology* **474**, 447–462.

Balke, C. W. & Shorofsky, S. R. (1998). Alterations in calcium handling in cardiac hypertrophy and heart failure. *Cardiovascular Research* **37**, 290–299.

Bassani, J. W., Bassani, R. A. & Bers, D. M. (1994). Relaxation in rabbit and rat cardiac cells: species-dependent differences in cellular mechanisms. *Journal of Physiology* **476**, 279–293.

Bassani, J. W., Yuan, W. & Bers, D. M. (1995). Fractional SR Ca release is regulated by trigger Ca and SR Ca content in cardiac myocytes. *American Journal of Physiology* **268**, C1313–1319.

Baylor, S. M. & Hollingworth, S. (1988). Fura-2 calcium transients in frog skeletal muscle fibres. *Journal of Physiology* **403**, 151–192 (published erratum appears in *Journal of Physiology* **407**, 616).

Bers, D. M. (1992). *Excitation-Contraction Coupling and Cardiac Contractile Force*, pp. 1–258. Kluwer Academic Press, Dordrecht, Netherlands.

Beuckelmann, D. J., Nabauer, M. & Erdmann, E. (1992). Intracellular calcium handling in isolated ventricular myocytes from patients with terminal heart failure. *Circulation* **85**, 1046–1055.

Beuckelmann, D. J., Nabauer, M. & Erdmann, E. (1993). Alterations of $K^+$ currents in isolated human ventricular myocytes from patients with terminal heart failure. *Circulation Research* **73**, 379–385.

Bouchard, R. A., Clark, R. B. & Giles, W. R. (1995). Effects of action potential duration on excitation-contraction coupling in rat ventricular myocytes. Action potential voltage-clamp measurements. *Circulation Research* **76**, 790–801.

Brooksby, P., Levi, A. J. & Jones, J. V. (1993). Investigation of the mechanisms underlying the increased contraction of hypertrophied ventricular myocytes isolated from the spontaneously hypertensive rat. *Cardiovascular Research* **27**, 1268–1277.

Cerbai, E., Barbieri, M., Li, Q. & Mugelli, A. (1994). Ionic basis of action potential prolongation of hypertrophied cardiac myocytes isolated from hypertensive rats of different ages. *Cardiovascular Research* **28**, 1180–1187.

Cleemann, L., Wang, W. & Morad, M. (1998). Two-dimensional confocal images of organization, density, and gating of focal $Ca^{2+}$ release sites in rat cardiac myocytes. *Proceedings of the National Academy of Sciences of the USA* **95**, 10984–10989.

Collier, M. L., Thomas, A. P. & Berlin, J. R. (1999). Relationship between L-type $Ca^{2+}$ current and unitary sarcoplasmic reticulum $Ca^{2+}$ release events in rat ventricular myocytes. *Journal of Physiology* **516**, 117–128.

Cordeiro, J., Litwin, S. & Bridge, J. (2000). Can NCX rapidly set the gain of EC coupling without directly triggering SR Ca release in the heart? *Biophysical Journal* **78**, A2202 (abstract).

Coulombe, A., Momtaz, A., Richer, P., Swynghedauw, B. & Coraboeuf, E. (1994). Reduction of calcium-independent transient outward potassium current density in DOCA salt hypertrophied rat ventricular myocytes. *Pflügers Archiv* **427**, 47–55.

Fabiato, A. (1985). Simulated calcium current can both cause calcium loading in and trigger calcium release from the sarcoplasmic reticulum of a skinned canine cardiac Purkinje cell. *Journal of General Physiology* **85**, 291–320.

Ferrier, G. R., Zhu, J., Redondo, I. M. & Howlett, S. E. (1998). Role of cAMP-dependent protein kinase A in activation of a voltage-sensitive release mechanism for cardiac contraction in guinea-pig myocytes. *Journal of Physiology* **513**, 185–201.

Fiset, C., Clark, R. B., Larsen, T. S. & Giles, W. R. (1997). A rapidly activating sustained $K^+$ current modulates repolarization and excitation–contraction coupling in adult mouse ventricle. *Journal of Physiology* **504**, 557–563.

Gomez, A. M., Valdivia, H. H., Cheng, H., Lederer, M. R., Santana, L. F., Cannell, M. B., McCune, S. A., Altschuld, R. A. & Lederer, W. J. (1997). Defective excitation-contraction coupling in experimental cardiac hypertrophy and heart failure. *Science* **276**, 800–806.

Gwathmey, J. K., Copelas, L., MacKinnon, R., Schoen, F. J., Feldman, M. D., Grossman, W. & Morgan, J. P. (1987). Abnormal intracellular calcium handling in myocardium from patients with end-stage heart failure. *Circulation Research* **61**, 70–76.

Hamill, O. P., Marty, A., Neher, E., Sakmann, B. & Sigworth, F. J. (1981). Improved patch-clamp techniques for high-resolution current recording from cells and cell-free membrane patches. *Pflügers Archiv* **391**, 85–100.

Han, S., Schiefer, A. & Isenberg, G. (1994). $Ca^{2+}$ load of guinea-pig ventricular myocytes determines efficacy of brief $Ca^{2+}$ currents as trigger for $Ca^{2+}$ release. *Journal of Physiology* **480**, 411–421.

Howlett, S. E., Zhu, J. Q. & Ferrier, G. R. (1998). Contribution of a voltage-sensitive calcium release mechanism to contraction in cardiac ventricular myocytes. *American Journal of Physiology* **274**, H155–170.

Isenberg, G. & Han, S. (1994). Gradation of $Ca^{2+}$-induced $Ca^{2+}$ release by voltage-clamp pulse duration in potentiated guinea-pig ventricular myocytes. *Journal of Physiology* **480**, 423–438.

Janczewski, A. M., Spurgeon, H. A., Stern, M. D. & Lakatta, E. G. (1995). Effects of sarcoplasmic reticulum $Ca^{2+}$ load on the gain function of $Ca^{2+}$ release by $Ca^{2+}$ current in cardiac cells. *American Journal of Physiology* **268**, H916–920.

Kaab, S., Nuss, H. B., Chiamvimonvat, N., O'Rourke, B., Pak, P. H., Kass, D. A., Marban, E. & Tomaselli, G. F. (1996). Ionic mechanism of action potential prolongation in ventricular myocytes from dogs with pacing-induced heart failure. *Circulation Research* **78**, 262–273.

Kaprielian, R., Wickenden, A. D., Kassiri, Z., Parker, T. G., Liu, P. P. & Backx, P. H. (1999). Relationship between $K^+$ channel down-regulation and $[Ca^{2+}]_i$ in rat ventricular myocytes following myocardial infarction. *Journal of Physiology* **517**, 229–245.

Levesque, P. C., Leblanc, N. & Hume, J. R. (1991). Role of reverse-mode $Na^+$-$Ca^{2+}$ exchange in excitation-contraction coupling in the heart. *Annals of the New York Academy of Sciences* **639**, 386–397.

Levi, A. J., Mitcheson, J. S. & Hancox, J. C. (1996). The effect of internal sodium and caesium on phasic contraction of patch-clamped rabbit ventricular myocytes. *Journal of Physiology* **492**, 1–19.

Litwin, S. E. & Bridge, J. H. (1997). Enhanced $Na^+$-$Ca^{2+}$ exchange in the infarcted heart. Implications for excitation-contraction coupling. *Circulation Research* **81**, 1083–1093.

Litwin, S. E., Li, J. & Bridge, J. H. (1998). Na-Ca exchange and the trigger for sarcoplasmic reticulum Ca release: studies in adult rabbit ventricular myocytes. *Biophysical Journal* **75**, 359–371.

Lopez-Lopez, J. R., Shacklock, P. S., Balke, C. W. & Wier, W. G. (1995). Local calcium transients triggered by single L-type calcium channel currents in cardiac cells. *Science* **268**, 1042–1045.

Nabauer, M., Beuckelmann, D. J., Uberfuhr, P. & Steinbeck, G. (1996). Regional differences in current density and rate-dependent properties of the transient outward current in subepicardial and subendocardial myocytes of human left ventricle. *Circulation* **93**, 168–177.

O'Rourke, B., Kass, D. A., Tomaselli, G. F., Kaab, S., Tunin, R. & Marban, E. (1999). Mechanisms of altered excitation-contraction coupling in canine tachycardia-induced heart failure, I: experimental studies. *Circulation Research* **84**, 562–570.

Page, E. (1978). Quantitative ultrastructural analysis in cardiac membrane physiology. *American Journal of Physiology* **235**, C147–158.

Piacentino, V. III & Houser, S. (2000). Reverse-mode $Na^+$-$Ca^{2+}$ exchange modulates SR $Ca^{2+}$ release caused by the L-type $Ca^{2+}$ current. *Biophysical Journal* **78**, A2206 (abstract).

Potreau, D., Gomez, J. P. & Fares, N. (1995). Depressed transient outward current in single hypertrophied cardiomyocytes isolated from the right ventricle of ferret heart. *Cardiovascular Research* **30**, 440–448.

Rose, W. C., Balke, C. W., Wier, W. G. & Marban, E. (1992). Macroscopic and unitary properties of physiological ion flux through L-type $Ca^{2+}$ channels in guinea-pig heart cells. *Journal of Physiology* **456**, 267–284.

Santana, L. F., Cheng, H., Gomez, A. M., Cannell, M. B. & Lederer, W. J. (1996). Relation between the sarcolemmal $Ca^{2+}$ current and $Ca^{2+}$ sparks and local control theories for cardiac excitation-contraction coupling. *Circulation Research* **78**, 166–171.

Santana, L. F., Kranias, E. G. & Lederer, W. J. (1997). Calcium sparks and excitation-contraction coupling in phospholamban-deficient mouse ventricular myocytes. *Journal of Physiology* **503**, 21–29.

Sham, J. S., Song, L. S., Chen, Y., Deng, L. H., Stern, M. D., Lakatta, E. G. & Cheng, H. (1998). Termination of $Ca^{2+}$ release by a local inactivation of ryanodine receptors in cardiac myocytes. *Proceedings of the National Academy of Sciences of the USA* **95**, 15096–15101.

Shorofsky, S. R., Aggarwal, R., Corretti, M., Baffa, J. M., Strum, J. M., Al-Seikhan, B. A., Kobayashi, Y. M., Jones, L. R., Wier, W. G. & Balke, C. W. (1999). Cellular mechanisms of altered contractility in the hypertrophied heart: big hearts, big sparks. *Circulation Research* **84**, 424–434.

Sipido, K. R., Maes, M. & Van de Werf, F. (1997). Low efficiency of $Ca^{2+}$ entry through the $Na^{+}$-$Ca^{2+}$ exchanger as trigger for $Ca^{2+}$ release from the sarcoplasmic reticulum. A comparison between L-type $Ca^{2+}$ current and reverse-mode $Na^{+}$-$Ca^{2+}$ exchange. *Circulation Research* **81**, 1034–1044.

Sipido, K. R. & Wier, W. G. (1991). Flux of $Ca^{2+}$ across the sarcoplasmic reticulum of guinea-pig cardiac cells during excitation–contraction coupling. *Journal of Physiology* **435**, 605–630.

Terracciano, C. M. & MacLeod, K. T. (1997). Measurements of $Ca^{2+}$ entry and sarcoplasmic reticulum $Ca^{2+}$ content during the cardiac cycle in guinea pig and rat ventricular myocytes. *Biophysical Journal* **72**, 1319–1326.

Terracciano, C. M., Tweedie, D. & MacLeod, K. T. (1997). The effects of changes to action potential duration on the calcium content of the sarcoplasmic reticulum in isolated guinea-pig ventricular myocytes. *Pflügers Archiv* **433**, 542–544.

Trafford, A. W., Diaz, M. E., Negretti, N. & Eisner, D. A. (1997). Enhanced $Ca^{2+}$ current and decreased $Ca^{2+}$ efflux restore sarcoplasmic reticulum $Ca^{2+}$ content after depletion. *Circulation Research* **81**, 477–484.

Varro, A., Negretti, N., Hester, S. B. & Eisner, D. A. (1993). An estimate of the calcium content of the sarcoplasmic reticulum in rat ventricular myocytes. *Pflügers Archiv* **423**, 158–160.

Wasserstrom, J. A. & Vites, A. M. (1996). The role of $Na^{+}$–$Ca^{2+}$ exchange in activation of excitation–contraction coupling in rat ventricular myocytes. *Journal of Physiology* **493**, 529–542.

Wettwer, E., Amos, G. J., Posival, H. & Ravens, U. (1994). Transient outward current in human ventricular myocytes of subepicardial and subendocardial origin. *Circulation Research* **75**, 473–482.

Wickenden, A. D., Kaprielian, R., Kassiri, Z., Tsoporis, J. N., Tsushima, R., Fishman, G. I. & Backx, P. H. (1998). The role of action potential prolongation and altered intracellular calcium handling in the pathogenesis of heart failure. *Cardiovascular Research* **37**, 312–323.

Wickenden, A. D., Kaprielian, R., Parker, T. G., Jones, O. T. & Backx, P. H. (1997). Effects of development and thyroid hormone on $K^{+}$ currents and $K^{+}$ channel gene expression in rat ventricle. *Journal of Physiology* **504**, 271–286.

Wier, W. G., Egan, T. M., Lopez-Lopez, J. R. & Balke, C. W. (1994). Local control of excitation–contraction coupling in rat heart cells. *Journal of Physiology* **474**, 463–471.

**Acknowledgements**

This study was supported by a Heart & Stroke Foundation of Ontario grant to P.H.B. R.S. is the recipient of a MD/PhD Studentship from the Medical Research Council of Canada, R.J.R. is the recipient of a Heart & Stroke/Richard Lewar Centre of Excellence Fellowship, R.K. holds an MRC Doctoral Research Award and P.H.B. is a Career Investigator of the Heart & Stroke Foundation of Ontario. We are grateful for equipment support from the Tiffin Trust Fund and the Centre for Cardiovascular Research at the University of Toronto.

**Corresponding author**

P. H. Backx: Toronto General Hospital, CCRW 3-802, 101 College Street, Toronto, Ontario, Canada M5G 2C4.

Email: p.backx@utoronto.ca